

Mott and Wigner-Mott transitions in doped correlated electron systems: effects of superlattice potential and inter-site correlation

Chunhua Li and Ziqiang Wang

Department of Physics, Boston College, Chestnut Hill, Massachusetts 02467

We introduce the notion of superstructure Mottness to describe the Mott and Wigner-Mott transition in doped strongly correlated electron systems at commensurate filling fractions away from one electron per site. We show that superstructure Mottness emerges in an inhomogeneous electron system when the superstructure contains an odd number of electrons per supercell. We argue that superstructure Mottness exists even in the absence of translation symmetry breaking by a superlattice, provided that the extended or intersite Coulomb interaction is strong. In the latter case, superstructure Mottness offers a unifying framework for the Mott and Wigner physics and a non-perturbative, strong coupling description of the Wigner-Mott transition. We support our proposal by studying a minimal single-band ionic Hubbard t - U - V - Δ model with nearest neighbor Coulomb repulsion V and a two-sublattice ionic potential Δ . The model is mapped onto a Hubbard model with two effective “orbitals” representing the two sites within the supercell, the intra and interorbital Coulomb repulsion U and $U' \sim V$, and a crystal field splitting Δ . Charge order on the original lattice corresponds to orbital order. Developing a cluster Gutzwiller approximation, we study the effects and the interplay between V and Δ on the Mott and Wigner-Mott transitions at quarter-filling. We provide the mechanism by which the superlattice potential enhances the correlation effects and the tendency towards local moment formation, construct and elucidate the phase diagram in the unifying framework of superstructure Mottness.

PACS numbers: 71.27.+a, 71.10.Fd, 71.30.+h

I. INTRODUCTION

The Mott physics, i.e. the transition from band to localized states due to interaction, plays an important role in materials containing strongly correlated electrons. The usual condition for Mott transition on a lattice requires half-filling, i.e. one electron per site. Due to Coulomb blocking, the electrons are localized and behave as local moments when the on-site Coulomb repulsion U becomes larger than the bandwidth of the kinetic energy. The transition metal oxides and rare earths and actinides, involving narrow bands from the atomic d and f orbitals, are known to exhibit Mottness – a remarkable set of electronic properties due to the proximity to Mott transition^{1,2}.

Thus far the study of Mott transition and the associated Mottness has mostly focused on uniform systems. In this paper, we propose and develop the notion of superstructure Mottness to describe the Mott physics for inhomogeneous electronic states. This is important because strongly correlated electron systems have a propensity towards inhomogeneous phases as a result of the frustrated kinetic energy. Examples include the transition metal chalcogenides that form charge density waves (CDW)^{3,4} and the high- T_c cuprates that exhibit stripe⁵ and checkerboard orders⁶. The superstructure in strongly correlated systems can also come from structural distortions as in Ca-substituted strontium ruthenates⁷ or chemical dopants as in the sodium cobaltates⁸.

Let us consider a commensurate superstructure in two dimensions with a $p \times q$ supercell. An electron density $n^* = \ell/pq$ corresponds to ℓ electrons per supercell. If ℓ is an odd integer, the condition for the superstructure Mott

transition is satisfied by an odd number of electrons per supercell. More precisely, for $\ell = 2k + 1$, k of the $M = pq$ subbands are completely filled, while the $(k + 1)$ -th subband, hosting one electron, is at half-filling and can undergo Mott transition. Note that partial filling of the subbands leading to the semi-metallic states, which usually happens close to integral filling near the top and bottom of the subbands for an even number of electrons per supercell, will not occur here for a generic superlattice potential. As a result, superstructure Mottness allows the Mott transition to occur far away from one electron per site. For example, electron correlation is expected to be weak in the sodium rich phases of Na_xCoO_2 because of the proximity to a band insulator at $x = 1$. To the contrary, strong correlation effects are observed, possibly due to the superstructures induced by Na dopants^{8,9,10,11} that allow superstructure Mottness. Another example is the recent observation of orbital selective Mott transition in $\text{Ca}_{2-x}\text{Sr}_x\text{RuO}_4$ near $x = 0.2$ ¹²; the d_{xy} orbital hosting 1.5 electrons becomes Mott localized due to the $\sqrt{2} \times \sqrt{2}$ superstructure induced by RuO_6 octahedral distortion⁷ such that there are 3 electrons per supercell. A third example is that the $\sqrt{13} \times \sqrt{13}$ CDW reconstruction on the surface of 1T-TaSe₂ leads to one electron per supercell and causes a Mott transition at low temperatures which has been observed recently by scanning tunneling spectroscopy⁴.

In addition to Mott localization, another paradigm in the physics of strong electronic correlation is Wigner crystallization which, in contrast, is due to strong long-range Coulomb interaction V that causes electrons to crystallize (charge order) by Coulomb jamming. The electron crystallization into a charge ordered Wigner lat-

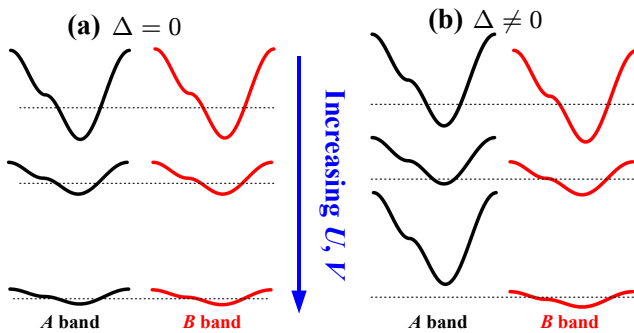


FIG. 1: (Color online) (a) and (b) Schematics of band evolution with interaction.

tice is another form of electronic superstructures. Wigner localization happens even classically for low density electrons in the continuum. What happens to lattice electrons when both U and V are large and away from half-filling, i.e. the Wigner-Mott transition, is largely unexplored theoretically because of the lack of nonperturbative many-body methods for treating the finite-range, inter-site Coulomb repulsion V . The basic difficulty is that the Hilbert space becomes nonlocal in the presence of the inter-site V , which defies the strong-coupling approaches based on the single-site Hilbert space containing four states representing an empty site, an up-spin electron, a down-spin electron, and a doubly occupied site. Previous approaches used a single-site Hilbert space Gutzwiller projection or dynamical mean field theory (DMFT) to treat the onsite U , but decoupled the inter-site V -term using the weak-coupling Hartree approximation^{13,14,15} which becomes unphysical when V is large since the electrons would avoid the high self-energy cost by not sitting close together.

It turns out that the notion of superstructure Mottness encompasses the physics of Wigner-Mott transition in a unified framework. Our basic insight is to envision the lattice as being covered by clusters or supercells and think of the latter as artificial atoms with a number of effective orbitals representing the sites contained in each cluster. This maps the problem to that of a multi-orbital Mott-Hubbard system where U and V play the role of intra- and inter-orbital interactions. Charge ordered states on the original lattice simply correspond to orbital order in the artificial atoms. This remarkable mapping, although approximate, allows us to treat the effects of V using the nonperturbative strong coupling approach for the multi-orbital Hubbard model and thus one is led to embrace a possible emergent Mott transition with increasing U and V at the filling fraction of one electron per cluster (supercell). Such a phenomenon of localization and local moment formation into clustered superstructures is another form of superstructure Mottness that unifies the Mott and Wigner physics.

The above picture amounts to truncating the nonlocal Hilbert space as a product of that of the clusters or super-

cells. The interactions between the electrons in the neighboring clusters are treated on equal footing. We extend the well established Gutzwiller projected wavefunction approach and develop a cluster Gutzwiller method. Explicit model calculations are performed to test the ideas of superstructure Mottness. Specifically, we study a minimal one-band, ionic Hubbard model with intersite correlations, i.e. the t - U - V - Δ model. In addition to the onsite Hubbard U and the nearest neighbor (NN) Coulomb interaction V , an onsite two-sublattice potential Δ_i is included for possible external potentials due to lattice distortion and dopant ions. We map the model to a generic two-orbital Hubbard model on a superlattice that contains two sites per supercell. The Hubbard U serves as the intra-orbital Coulomb U ; the inter-site V becomes the inter-orbital repulsion $U' = V$, whereas the superlattice potential Δ_i turns into an effective crystal field Δ_α , with $\alpha = A, B$ labeling the two ‘‘atomic’’ orbitals with a crystal field splitting $\Delta = \Delta_A - \Delta_B$. Using the cluster Gutzwiller projection of the multioccupancy states in a supercell, in analogy to the multiorbital Gutzwiller projection method¹⁶, we study the ground state phase diagram at quarter filling in the parameter space of U , V , and Δ . Fig. 1 shows the schematics of two classes of localization transitions with increasing U and V . For $\Delta = 0$, the two bands remain degenerate and undergo the transition simultaneously from a uniform correlated metal to a Mott insulator without charge (i.e. orbital) ordering. For $\Delta \neq 0$, we find a transition from a CDW metal involving both bands to a charge ordered insulator, where one of the two bands undergoes an orbital selective Mott transition¹⁷. We elucidate the mechanism by which the superlattice potential enhances the correlation effects and the tendency towards local moment formation, and reveal a deeper connection among the strongly correlated inhomogeneous electronic states, the Wigner-Mott physics, and the multiorbital Mott physics that can all be united under the notion of superstructure Mottness.

The rest of the paper is organized as follows. In section II, we discuss the model and the mapping to an equivalent multiorbital Hubbard model on the superstructure. In section III, we describe the virtual cluster Gutzwiller approximation (VCGA) and study the superstructure Mott transition in the ionic Hubbard model, i.e. the t - U - Δ model at quarter-filling, in the absence of inter-site Coulomb correlation V . In section IV, we extend the VCGA to the case of finite inter-site correlation V and study the Wigner-Mott transition in the absence of the ionic potential Δ , i.e. the t - U - V model at quarter-filling, using the ideas of superstructure Mottness. The results will be compared to the weak-coupling Hartree approximation. The general case of finite Δ and V is presented in section V followed by a brief summary in section VI.

II. MODEL AND HEURISTIC DISCUSSION

The Hamiltonian of the t - U - V - Δ model is given by

$$\hat{H} = - \sum_{i,j} (t_{ij} - \Delta_i \delta_{ij}) c_{i\sigma}^\dagger c_{j\sigma} + U \sum_i \hat{n}_{i\uparrow} \hat{n}_{i\downarrow} + V \sum_{\langle i,j \rangle} \hat{n}_i \hat{n}_j, \quad (1)$$

where $c_{i\sigma}^\dagger$ creates an electron at site i of spin σ on a square lattice. We consider electron hoppings between NN $t_{\langle i,j \rangle} = t$ and next NN $t_{\langle\langle i,j \rangle\rangle} = t'$. Repeated spin indices are summed. Eq. (1) is an extended version of the ionic Hubbard model with NN intersite repulsion V and a lattice ionic potential Δ_i . We focus on the simplest case where Δ_i , when present, has a superstructure with two-sites per supercell.

Consider the lattice as a complete coverage by a two-sublattice (A and B) superstructure. The two sites per supercell (cluster) can be viewed as two effective orbitals. The hopping terms can be written in the equivalent form of two bands having dispersions $\xi_{\alpha\alpha}(k) = -2t'(\cos k_x + \cos k_y)$ with an inter-band ($\alpha \neq \beta$) hopping $\xi_{\alpha\beta} = -4t \cos(k_x/2) \cos(k_y/2)$, where $\alpha, \beta = A, B$ label the two orbitals and $k \in$ the reduced Brillouin zone of the reciprocal lattice. The Hamiltonian can be rewritten in a suggestive form

$$\begin{aligned} \hat{H} = & \sum_{\alpha,\beta,k} \xi_{\alpha\beta}(k) c_{k,\alpha\sigma}^\dagger c_{k,\beta\sigma} + U \sum_{\alpha,I} \hat{n}_{I,\alpha\uparrow} \hat{n}_{I,\alpha\downarrow} \\ & + \sum_{\alpha,I} \Delta_\alpha \hat{n}_{I,\alpha} + U' \sum_I \hat{n}_{I,A} \hat{n}_{I,B} \\ & + V' \sum'_{(I,J)} \hat{n}_{I,A} \hat{n}_{J,B}. \end{aligned} \quad (2)$$

where the sum over I runs over the supercells on the lattice. Eq. (2) has the generic form of a two-band Hubbard model with the onsite intra-orbital Coulomb repulsion U and the inter-orbital Coulomb repulsion $U' = V$. The superlattice potential Δ_α plays the role of a crystal field and gives rise to a crystal field splitting $\Delta = \Delta_A - \Delta_B$. The last term with $V' = V$ accounts for the inter-orbital Coulomb interaction between the neighboring supercells. Note that the U and U' are free parameters in our theory and not related by the Hund's rule coupling J_H in contrast to the usual multiorbital Hubbard model¹⁸.

III. SUPERSTRUCTURE MOTT TRANSITION IN THE IONIC HUBBARD MODEL $\Delta \neq 0$, $V = 0$

We first focus on the ionic Hubbard model in the absence of the inter-site Coulomb correlation ($V = 0$). The correlation effects will be treated by the Gutzwiller projected wavefunctions. We first review briefly this variational wavefunction approach to the Hubbard model and the Gutzwiller approximation as a semi-analytical method to carry out the projection. The virtual cluster Gutzwiller approximation will then be introduced to

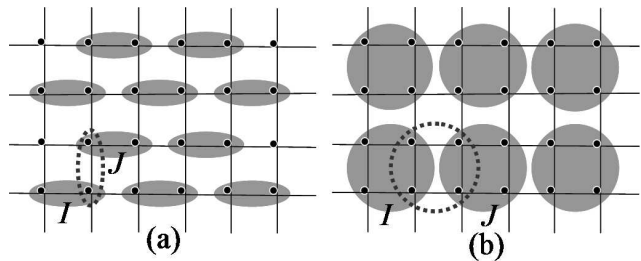


FIG. 2: Dividing the original lattice into clusters. The dark dots represent the original lattice sites while the gray areas are the clusters, (a) a two-site supercell and (b) a four-site supercell. Here I and J label the position of each cluster. The dotted circles represent equivalent selection of the supercells.

treat the superlattice modulations induced by the ionic potential $\Delta_i \neq 0$.

A. Gutzwiller approximation to the Hubbard Model

For the Hubbard model with only onsite repulsion U , the Hilbert space is a direct product of the single-site Fock states: one empty, two singly occupied (either by an up or a down spin), and one doubly occupied. The Gutzwiller projected wavefunction approach is a way of building correlation effects from the non-interacting wavefunctions by reducing the statistical weight of double occupation¹⁹. The trial wavefunction can be written down formally as $|\Psi\rangle = \hat{P}|\Psi_0\rangle$, with $|\Psi_0\rangle$ being the non-interacting Slater determinant wavefunction and \hat{P} the Gutzwiller projection operator. The projection operator $\hat{P} = g^{\hat{D}}$, where $\hat{D} = \sum_i \hat{n}_{i\uparrow} \hat{n}_{i\downarrow}$ is the double occupation operator of the system and $g \leq 1$ a variational parameter to be determined by minimizing the ground state energy $\langle \Psi | \hat{H} | \Psi \rangle / \langle \Psi | \Psi \rangle$, the average interaction energy is simply given by Ud , with d being the average density of double occupancy. Since there is a one to one correspondence between d and g , one can make d the variational parameter instead of g . The task is then to derive an expression for the kinetic energy in terms of d . Unfortunately, an analytical expression for this expectation value is not available other than in one and infinite dimensions²⁰. In two and three dimensions one has to resort to approximate methods. The Gutzwiller approximation relates the expectation values in the projected state with that of the uncorrelated state by a simple multiplicative factor, the Gutzwiller factor (GF). This is achieved by ignoring inter-site correlations in evaluating the expectation values with $|\Psi\rangle$,

$$\langle \Psi | \sum_{i,j} c_{i\sigma}^\dagger c_{j\sigma} | \Psi \rangle / \langle \Psi | \Psi \rangle \approx g_\sigma^2 \langle \Psi_0 | \sum_{i,j} c_{i\sigma}^\dagger c_{j\sigma} | \Psi_0 \rangle, \quad (3)$$

where g_σ is the GF for the kinetic hopping term and translational invariance of the lattice is assumed. The exact form of g_σ depends on the trial wavefunction $|\Psi_0\rangle$ and can be obtained by considering how double occupation affects the hopping process. If $|\Psi_0\rangle$ is taken as the Slater determinant state without further symmetry breaking, g_σ takes a simple form in terms of the uniform particle density and the density of double occupation^{21,22},

$$g_\sigma = \left[\frac{(n_\sigma - d)(1 + d - n)}{n_\sigma(1 - n_\sigma)} \right]^{1/2} + \left[\frac{d(n_{\bar{\sigma}} - d)}{n_\sigma(1 - n_\sigma)} \right]^{1/2}. \quad (4)$$

As a result, the minimization of the ground state energy for the original Hubbard Hamiltonian translates to the minimization of the following renormalized mean field Hamiltonian,

$$\hat{H}_{\text{GA}} = - \sum_{i,j} g_\sigma^2 t_{ij} c_{i\sigma}^\dagger c_{j\sigma} + \sum_{i\sigma} \lambda_\sigma (\hat{n}_{i\sigma} - n_\sigma) + NUd, \quad (5)$$

where the hopping integrals are renormalized by a factor of g_σ^2 from the original ones. Here N is the number of sites and λ_σ is a Lagrange multiplier that keeps the particle density unchanged before and after the projection. Under the Gutzwiller approximation, the ground state energy of the original Hubbard model is approximated by that of the mean field Hamiltonian \hat{H}_{GA} . The correlation effects are treated nonperturbatively since there are no self-energy corrections that scale with U in contrast to the weak coupling Hartree-Fock approach. Since the bandwidth (hopping) is renormalized in \hat{H}_{GA} , this approach is also known as the renormalized mean field approximation²³.

B. The Virtual Cluster Gutzwiller Approximation

Several authors have extended the original Gutzwiller approximation to handle lattice translational symmetry breaking using different schemes^{24,25,26,27}. In the spatially unrestricted Gutzwiller approximation (SUGA)^{24,28}, the GF for the hopping renormalization is generalized to depend on the local charge densities and double occupations at the sites connected by the hopping process. Specifically, $g_{ij\sigma}$ for the hopping from site i to site j is a product $g_{i\sigma} \cdot g_{j\sigma}$, with $g_{i\sigma}$ given by

$$g_{i\sigma} = \left[\frac{(n_{i\sigma} - d_i)(1 + d_i - n_i)}{n_{i\sigma}(1 - n_{i\sigma})} \right]^{1/2} + \left[\frac{d_i(n_{i\bar{\sigma}} - d_i)}{n_{i\sigma}(1 - n_{i\sigma})} \right]^{1/2}, \quad (6)$$

where d_i is the double occupation at site i , $n_{i\sigma}$ is the spin dependent density, and $n_i = \sum_\sigma n_{i\sigma}$. The latter has spatial modulations due to the presence of superlattice potential Δ_i . The Mott transition in a given superstructure at appropriate filling fractions can be analyzed using the SUGA and the GF in Eq. (6).

In order to gain more physical insights into the problem and establish the notion of superstructure Mottness,

A	—	↑	↓	—	—	↑↓	—	↑
B	—	—	—	↑	↓	—	↑↓	↑
prob.	e	$p_{A\uparrow}$	$p_{A\downarrow}$	$p_{B\uparrow}$	$p_{B\downarrow}$	d_{AA}	d_{BB}	$d_{\uparrow\uparrow}$
int. eng.	0	0	0	0	0	U	U	V
A	↑	↓	↓	↑	↓	↑↓	↑	↑
B	↓	↑	↓	↑↓	↑↓	↑	↓	↑
prob.	$d_{\downarrow\downarrow}$	$d_{\downarrow\uparrow}$	$d_{\downarrow\downarrow}$	$t_{A\uparrow}$	$t_{A\downarrow}$	$t_{B\uparrow}$	$t_{B\downarrow}$	f
int. eng.	V	V	V	E_T	E_T	E_T	E_T	E_F

FIG. 3: (Color online) The local Fock space of a two-site cluster. The expectation probability of each state and the corresponding interaction energy are also given. Here $E_T = U + 2V$ and $E_F = 2U + 4V$.

we develop a virtual cluster approach. For a periodic superlattice potential $\Delta_i \neq 0$, the original lattice is divided into supercells. It is important to note that there are many equivalent ways to choose the supercell clusters that cover the whole lattice. A particular two-site supercell and a four-site supercell coverage of the original lattice is shown in Figs. 2(a) and 2(b). Thus, a lattice site is labeled by (I, i) where the capital letter I specifies the supercell and i denotes the position inside the supercell. The Hamiltonian in Eq. (1) can be written as $\hat{H} = \hat{H}_K + \hat{H}_{\text{local}}$, where the “kinetic” part \hat{H}_K and the “local” interaction part \hat{H}_{local} are given by,

$$\hat{H}_K = - \sum_{I,i;J,j} t_{ij} c_{Ii\sigma}^\dagger c_{Jj\sigma}, \quad (7a)$$

$$\hat{H}_{\text{local}} = U \sum_{I,i} \hat{n}_{Ii\uparrow} \hat{n}_{Ii\downarrow} + \sum_{I,i} \Delta_i \hat{n}_{Ii}. \quad (7b)$$

In the spirit of Gutzwiller projected wavefunction, the effect of \hat{H}_{local} is to reduce multi-occupation in each supercell. For example, the Fock states of a two-site supercell are shown in Fig. 3, where 11 of the 16 states in a cluster have more than one particle. The operators for these multiplets are denoted by $\hat{\mathbb{M}}_\gamma$, $\gamma = 1, \dots, \Gamma$, with Γ the dimension of the multi-occupancy space ($\Gamma = 11$ in the two-site cluster example). A trial wavefunction can then be written as $|\Psi\rangle = \hat{P}|\Psi_0\rangle$, where the projection operator \hat{P} is a product of the cluster projection operators, \hat{P}_I , i.e., $\hat{P} = \prod_I \hat{P}_I$. The cluster projection operator \hat{P}_I reduces multi-occupation within each cluster I and is written down as,

$$\hat{P}_I = \prod_{i\sigma} y_{i\sigma}^{\hat{n}_{i\sigma}} \cdot \prod_{\gamma=1}^{\Gamma} g_\gamma^{\hat{\mathbb{M}}_\gamma}, \quad (8)$$

where the supercell index I is omitted on the right hand side because of translation symmetry on the superlattice. Here the y 's are fugacities that keep charge densities unchanged upon projection at each site and the g_γ 's are

variationally determined weighting factors for the projection.

The hopping processes in Eq. (7a) is then renormalized by the projected wave function as in Eq. (3) and the GF is calculated by ignoring inter-cell correlations. However, it is important to note that for a fixed choice of a supercell coverage of the lattice, \hat{H}_K includes hopping between different supercells/clusters ($I \neq J$) as well as hopping within the same cluster ($I = J$). Conventional cluster approaches, such as the one used by Lechermann et al., do fix the choice of the supercells. This, however, leads unavoidably to dimerization since the inter-cluster hopping and intra-cluster hopping cannot be treated on equal footing and acquire different renormalization factors²⁹. Here we propose a *virtual cluster* approach. We do not fix a real space cluster coverage of the lattice in *a priori*. Instead, the choice of the clusters is associated with the Hilbert space and arises when evaluating the expectation values of the hopping terms using the projected wavefunction in Eq. (3). Indeed, in order to implement the Gutzwiller approximation, the hopping term must be between different clusters (i.e. inter-cluster) and the correlation between the clusters must be ignored. Our insight is that for any two sites connected by the hopping process on the original lattice, one can always find a particular choice of supercell coverage such that the two sites reside in two different supercells. As an example, choosing the cluster marked by the dotted circles in Figs. 2(a) and 2(b) turns the sites within the cluster (gray) into ones residing in different supercells.

Specifically, consider the hopping terms in Eq. (7a). In the term where $I = J$, it is always possible to choose an equivalent cluster coverage such that the hopping is between sites in different clusters $I' \neq J'$. When evaluating the expectation value of this hopping term using the projected wave function, one can simply rearrange the product of the cluster Fock states and write $\hat{P} = \prod_{I'} \hat{P}_{I'}$ and arrive at the same result as the case when $I \neq J$. It is in this sense, we term this approach as the virtual cluster Gutzwiller approximation (VCGA). One of the most notable advantages of this approach is that the same Gutzwiller renormalization factor is obtained for the hopping integral between any two sites regardless of the choice of the supercell coverage of the original lattice and, as a result, the difficulty associated with the unphysical dimerization tendency is removed.

The remaining steps for deriving the GF is the same as that of the multi-orbital Hubbard model with only on-site density-density interactions¹⁶. In this sense, one can regard each supercell as an artificial ‘‘atom’’ and the lattice sites within the cluster as the associated atomic ‘‘orbitals’’, and we will use orbitals and sites within a

cluster interchangeably. We obtain

$$\begin{aligned} \langle c_{I\alpha\sigma}^\dagger c_{J\beta\sigma} \rangle &= \frac{\langle \hat{P}_I c_{I\alpha\sigma}^\dagger \hat{P}_I \hat{P}_J c_{J\beta\sigma}^\dagger \hat{P}_J \rangle_0}{\langle \hat{P}_I^2 \hat{P}_J^2 \rangle_0} \\ &= \frac{\langle \hat{\mathbb{W}}_{I\alpha\sigma} \hat{\mathbb{W}}_{J\beta\sigma} \rangle_0}{\langle \hat{P}_I^2 \hat{P}_J^2 \rangle_0} \cdot \langle c_{I\alpha\sigma}^\dagger c_{J\beta\sigma} \rangle_0 \\ &= \frac{\langle \hat{\mathbb{W}}_{I\alpha\sigma} \rangle_0 \langle \hat{\mathbb{W}}_{J\beta\sigma} \rangle_0}{\langle \hat{P}_I^2 \rangle_0 \langle \hat{P}_J^2 \rangle_0} \cdot \langle c_{I\alpha\sigma}^\dagger c_{J\beta\sigma} \rangle_0 \\ &= g_{I\alpha\sigma} g_{J\beta\sigma} \langle c_{I\alpha\sigma}^\dagger c_{J\beta\sigma} \rangle_0, \end{aligned} \quad (9)$$

where $\langle \dots \rangle_0$ denotes expectation values in the unprojected state $|\Psi_0\rangle$ and the equalities hold only when inter-cluster correlations are ignored in the spirit of the Gutzwiller approximation. Here $\hat{\mathbb{W}}_{I\alpha\sigma}$ is defined as,

$$\hat{\mathbb{W}}_{I\alpha\sigma} c_{I\alpha\sigma}^\dagger = \hat{P}_I c_{I\alpha\sigma}^\dagger \hat{P}_I, \quad (10)$$

and $g_{I\alpha\sigma} = \langle \hat{\mathbb{W}}_{I\alpha\sigma} \rangle_0 / \langle \hat{P}_{I\alpha\sigma}^2 \rangle_0$. Because of translational symmetry of the superlattice, $g_{I\alpha\sigma}$ is independent of the supercell index I , i.e., $g_{I\alpha\sigma} = g_{\alpha\sigma}$.

In the rest of this section we focus on a two-site cluster on a square lattice, compatible with a superlattice potential

$$\Delta_i = \frac{\Delta}{2} (-1)^{i_x + i_y}. \quad (11)$$

The two sites inside a cluster, i.e. the two orbitals are labeled as A and B . The Δ in the above equation has the meaning of a crystal field splitting between the orbitals. The multi-occupation projection operators \mathbb{M}_γ 's are as follows (suppressing the supercell index), $\hat{D}_{\alpha\alpha} = \hat{D}_\alpha \hat{E}_{\bar{\alpha}}$ – intraorbital doublon projection operator for the state with a doubly occupied α orbital (created by \hat{D}_α) and an empty orbital (created by $\hat{E}_{\bar{\alpha}}$); $\hat{D}_{\sigma\sigma'} = \hat{Q}_{\alpha\sigma} \hat{Q}_{\bar{\alpha}\sigma'}$ – interorbital doublon projection operator for the state with two singly occupied orbitals of spin projections σ (created by $\hat{Q}_{\alpha\sigma}$) and σ' (created by $\hat{Q}_{\bar{\alpha}\sigma'}$); $\hat{T}_{\alpha\sigma} = \hat{Q}_{\alpha\sigma} \hat{D}_{\bar{\alpha}}$ – triplon projection operator for the state with a singly occupied α orbital with spin σ and a doubly occupied orbital; and $\hat{F} = \hat{D}_\alpha \hat{D}_{\bar{\alpha}}$ – quadruplon projection operator for the state with both orbitals doubly occupied. The projection operators for singly occupied states are denoted by $\hat{P}_{\alpha\sigma}$ where the α orbital with spin σ is occupied while the other orbital is empty, and projecting to the configuration where both orbitals are empty is accomplished by $\hat{E} = \hat{E}_\alpha \hat{E}_{\bar{\alpha}}$. The expectation values of these operators in the projected state will be denoted by a lower case letter. For example, $\langle \hat{T}_{\alpha\sigma} \rangle = t_{\alpha\sigma}$, see Fig. 3. The definition of the single-orbital projection operators are the doubly occupied $\hat{D}_\alpha = \hat{n}_{\alpha\uparrow} \hat{n}_{\alpha\downarrow}$, singly occupied $\hat{Q}_{\alpha\sigma} = \hat{n}_{\alpha\sigma} (1 - \hat{n}_{\alpha\bar{\sigma}})$ and empty orbital $\hat{E}_\alpha = (1 - \hat{n}_{\alpha\uparrow})(1 - \hat{n}_{\alpha\downarrow})$. The expectation values of these single-orbital projection operators in the projected states are also denoted by a lower case letter, e.g., $\langle \hat{Q}_{\alpha\sigma} \rangle = q_{\alpha\sigma}$. It is seen from Eq. (9) that the GF, $g_{\alpha\sigma}$, depends on the

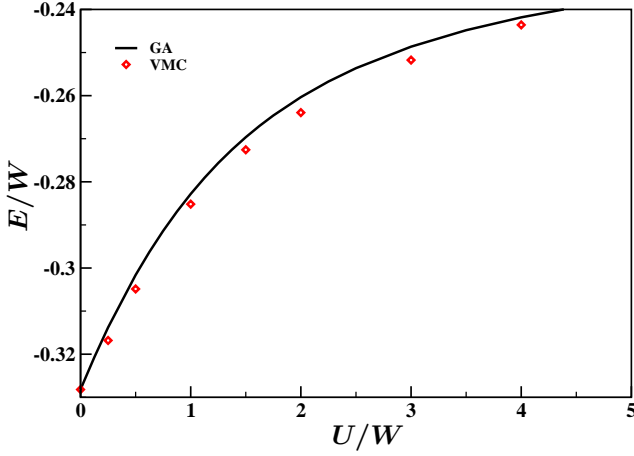


FIG. 4: (Color online) Comparison of ground state energy of the Hubbard model at quarter filling treated with Gutzwiller approximation and variational Monte Carlo³⁰. $V = \Delta = 0$, $W = 4t$.

fugacities $y_{\alpha\sigma}$ and g_γ . By expressing $y_{\alpha\sigma}$ and g_γ in terms of the occupation probabilities, we obtain the Gutzwiller factors²⁸,

$$g_{A\sigma} = \left(\sqrt{e p_{A\sigma}} + \sqrt{d_{AA} p_{A\bar{\sigma}}} + \sqrt{d_{\sigma\sigma} p_{B\sigma}} + \sqrt{d_{\sigma\bar{\sigma}} p_{B\bar{\sigma}}} \right. \\ \left. + \sqrt{d_{BB} t_{A\sigma}} + \sqrt{d_{\sigma\sigma} t_{B\sigma}} + \sqrt{d_{\sigma\bar{\sigma}} t_{B\bar{\sigma}}} + \sqrt{t_{A\bar{\sigma}} f} \right) \\ / \sqrt{n_{A\sigma}(1 - n_{A\sigma})}, \quad (12a)$$

$$g_{B\sigma} = \left(\sqrt{e p_{B\sigma}} + \sqrt{d_{BB} p_{B\bar{\sigma}}} + \sqrt{d_{\sigma\sigma} p_{A\sigma}} + \sqrt{d_{\sigma\bar{\sigma}} p_{A\bar{\sigma}}} \right. \\ \left. + \sqrt{d_{AA} t_{B\sigma}} + \sqrt{d_{\sigma\bar{\sigma}} t_{A\sigma}} + \sqrt{d_{\sigma\sigma} t_{A\bar{\sigma}}} + \sqrt{t_{B\bar{\sigma}} f} \right) \\ / \sqrt{n_{B\sigma}(1 - n_{B\sigma})}. \quad (12b)$$

In addition, the occupation probabilities satisfy the following constraints,

$$p_{A\sigma} = n_{A\sigma} - d_{AA} - \sum_{\sigma'} d_{\sigma\sigma'} - t_{A\sigma} - \sum_{\sigma'} t_{B\sigma'} - f, \quad (13a)$$

$$p_{B\sigma} = n_{B\sigma} - d_{BB} - \sum_{\sigma'} d_{\sigma'\sigma} - t_{B\sigma} - \sum_{\sigma'} t_{A\sigma'} - f, \quad (13b)$$

$$e = 1 - \sum_{\alpha} n_{\alpha} + \sum_{\alpha} d_{\alpha\alpha} + \sum_{\sigma\sigma'} d_{\sigma\sigma'} + 2 \sum_{\alpha,\sigma} t_{\alpha\sigma} + 3f, \quad (13c)$$

where Eqs. (13a) and (13b) are just alternative expressions of the electron densities in terms of the occupation probabilities and Eq. (13c) is the completeness of the *cluster* Fock states. These results are consistent with those obtained for the multiorbital Hubbard model¹⁶.

As an important check for the validity of the VCGA, we verified that the expressions in Eqs. (12a) and (12b) are equivalent to the results from the SUGA when inter-site correlations are ignored. To show this, one can make use of the fact that in the absence of inter-site correlations the multi-occupation probabilities in the virtual cluster approach are simple products of the occupation probabilities in SUGA. For example, the above defined triple-occupation $t_{A\sigma}$ is the product of the double occupation d_B and single occupation $q_{A\sigma}$, i.e. $t_{A\sigma} = d_B \cdot q_{A\sigma}$. By substituting all the multi-occupation probabilities in Eqs. (12a and 12b) one recovers the results given in Eq. (6).

C. Superstructure Mott Transition in the Ionic Hubbard Model

We next present the results for the ionic Hubbard model obtained with the VCGA at quarter filling for the superlattice potential of Eq. (11). Since the system is far away from half filling, no magnetic instability is present and we will focus on the paramagnetic solutions. The effective Hamiltonian in the VCGA discussed above is given by,

$$\hat{H}_{GA} = \sum_{k,\alpha\beta} g_{\alpha\sigma} g_{\beta\sigma} \xi_{\alpha\beta}(k) c_{k,\alpha\sigma}^\dagger c_{k,\beta\sigma} + \sum_{k,\alpha} \Delta_{\alpha} \hat{n}_{k,\alpha} \\ + N_c U \left(\sum_{\alpha} d_{\alpha\alpha} + \sum_{\alpha\sigma} t_{\alpha\sigma} + 2f \right) + \sum_{k,\alpha\sigma} \lambda_{\alpha\sigma} (\hat{n}_{k,\alpha\sigma} - n_{\alpha\sigma}), \quad (14)$$

where N_c is the number of clusters and $\lambda_{\alpha\sigma}$'s are the Lagrange multipliers that keep the particle density in each orbital unchanged following the projection. They originate from and have a one to one correspondence to the fugacities in the projection operator in Eq. (8). The ground state properties are determined by minimizing $\langle \hat{H}_{GA} \rangle$ and solving for $(e, p_{\alpha\sigma}, d_{\alpha\alpha}, d_{\sigma\sigma'}, t_{\alpha\sigma}, f)$ and $\lambda_{\alpha\sigma}$ self-consistently.

To test the algorithm, we first compute the ground state energy per site at quarter-filling as a function of U/W , where $W = 4t$ is the half-bandwidth, for the Hubbard model (i.e. set $\Delta = 0$). Fig. 4 shows that the later agrees remarkably well with the results obtained using the variational Monte Carlo method to carry out the projection³⁰. From the perspective of superstructure Mottness, it is clearly seen from Eq. (14) that the U term alone does not reduce the interorbital double occupancy $d_{\sigma\sigma'}$. As a consequence, U alone cannot drive a Mott transition away from half filling since the Gutzwiller factors in Eqs. (12a) and (12b) are always finite and the system is in a correlated metallic phase.

Switching on $\Delta \neq 0$, we determined the phase diagram of the ionic Hubbard model shown in Fig. 5(a) on the U - Δ plane where a CDW metal at small (U, Δ) and a charge ordered insulator for large (U, Δ) are separated by a continuous superstructure Mott metal-insulator transition. The notion of superstructure Mottness offers a

physical explanation of the phase structure through the analogy to multi-orbital Mott-Hubbard systems. A finite crystal field splitting Δ induces orbital order $n_A \neq n_B$, which corresponds to charge ordering in the ionic Hubbard model. However, below a critical strength of Δ , as seen in Fig. 5(a), the system remains in a metallic charge density wave (CDW) state no matter how strong U is. This can be understood since the two bands derived from the two orbitals are not separated in this case and the inter-orbital hopping is not suppressed due to the absence of an inter-orbital repulsion U' , which is related to the inter-site correlation V as shown in Eq. (2).

A sufficiently large crystal field splitting Δ drives the system from a CDW metal to a charge ordered insulating state for large enough U . This happens because the two bands gradually separate with increasing orbital polarization $\delta n = n_B - n_A$. The lower band becomes half-filled since the system is at quarter-filling. A large enough U drives a Mott transition in the half-filled lower quasiparticle (QP) band. Indeed, as $n_A \rightarrow 0$ and $p_{A\sigma} \rightarrow 0$, Eq. (13a) implies that all the double occupancies approach zero. This leads to $e \rightarrow 0$ at quarter filling from Eq. (13c). On the other hand, $n_B \neq 0$ such that from Eq. (12b) the Gutzwiller factor $g_{B\sigma} \rightarrow 0$ resulting in an orbital selective Mott transition shown in Fig. 5(d). In Figs. 5(b), 5(c), the doublon densities and the inverse effective mass of the lower QP band m/m^* , which equals the QP spectral weight Z , are plotted as a function of Δ at a fixed large $U = 3W$. The continuous transition at $\Delta_c = 2.4W$ is a Brinkman-Rice type transition³¹. The vanishing of the coherent QP spectral weight and the divergence of the effective mass (case shown in Fig. 1(b)) on approaching the transition from the metallic side are clear signatures of Mottness.

The curvature of the phase boundary at large ionic potential Δ can also be understood. In this regime, the crystal field splitting is much larger than the hopping t and the bands are well separated. A simple calculation shows that the bandwidth w of the lower QP band decreases with increasing Δ , $w \sim t^2/\Delta$. As a result, the critical U_c for the Mott transition, which depends on the ratio of U/w , decreases as can be seen in the phase diagram Fig. 5(a). The evolution of the QP band dispersion as a function of Δ is shown in Fig. 5(d) at fixed large $U = 3W$. It clearly demonstrates that the Mott transition in the ionic Hubbard model belongs to class (b) of the superstructure Mottness depicted in Fig. 1.

While the NN hopping t translates into interband hopping in the two-band model, the NNN hopping t' describes intraband hopping. We find that including a $t' = -0.2t$ moves the phase boundary toward smaller (Δ, U) , as can be seen in Fig. 5(d) where a continuous transition takes place at a smaller $\Delta_c = 1.9W$.

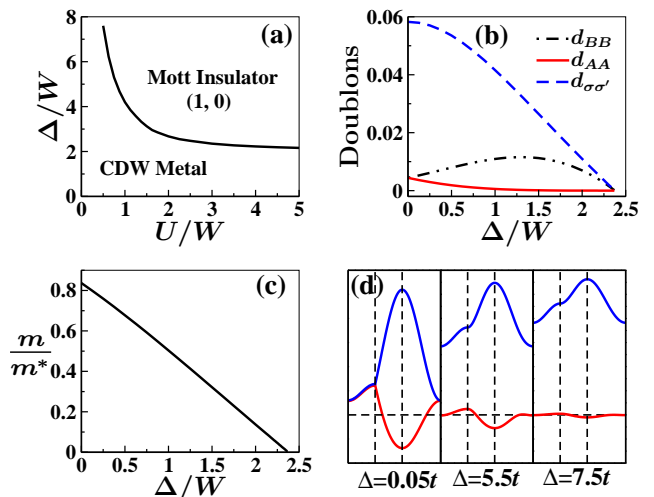


FIG. 5: (Color online) (a) Phase diagram on the U - Δ plane for $V = 0$ and $t' = 0$. Doublon densities (b) and inverse effective mass (c) as function of Δ for fixed $U = 3W$. (d) Band dispersion for different Δ , $t' = -0.2t$. $k = (\pi, 0) \rightarrow (\pi/2, \pi/2) \rightarrow (0, 0) \rightarrow (\pi, 0)$.

IV. SUPERSTRUCTURE MOTTNESS IN THE t - U - V MODEL

In this section, we study the superstructure Mott transition due to the inter-site Coulomb interaction V in the extended Hubbard, or the t - U - V model. To this end, the superlattice potential Δ is set to zero. Superstructure Mottness in the presence of both V and Δ will be studied in the next section. The basic difficulty introduced by the inter-site interaction V is that the Hilbert space becomes nonlocal, making it inaccessible to the conventional Gutzwiller projected wavefunction. We show that the VCGA offers a natural nonperturbative treatment of the Wigner-Mott transition within the framework of superstructure Mottness.

A. Virtual cluster Gutzwiller approximation for the V -term

In the Gutzwiller approach, one would like to treat the interactions as a projection that reduces multi-occupation from an unprojected Slater-determinate state, i.e. $|\Psi\rangle = \hat{P}|\Psi_0\rangle$. However, the projection operator \hat{P} cannot be written down in closed form, since the Hilbert space is infinitely connected by the inter-site V in Eq. (1). Our strategy is to truncate the nonlocal Hilbert space as a product of that of the supercell clusters such that the U and V within a cluster serve as the intra-orbital U and inter-orbital U' just as in a multi-orbital Hubbard model, which can be treated nonperturbatively. The projection operator \hat{P} can thus be written approximately as the product of the cluster projection operators,

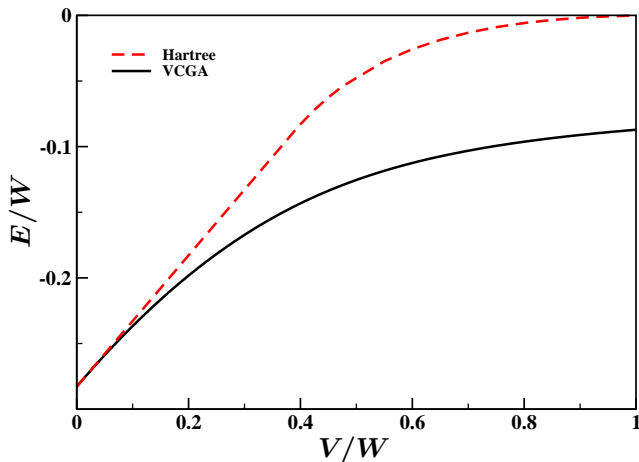


FIG. 6: (Color online) Comparison of the ground state energy obtained by VCGA and Hartree approximation of V -term at $U = W$.

\hat{P}_I , i.e., $\hat{P} = \prod_I \hat{P}_I$. This algorithm can be accomplished by the VCGA for the ionic Hubbard model discussed in section III.A, with a few extensions.

Although we do not fix a specific supercell structure in the virtual cluster approach, it is useful to write down the Hamiltonian for a given coverage of the lattice. Due to the non-local nature of the V -term, the interaction part of the Hamiltonian can no longer be written as a direct summation over independent supercells. Let us write the Hamiltonian as the sum of two parts, similar to Eqs. (7a) and (7b),

$$\hat{H}_K = - \sum_{I,i;J,j;\sigma} t_{ij} c_{Ii\sigma}^\dagger c_{Jj\sigma} \quad (15a)$$

$$\hat{H}_{\text{inter}} = U \sum_{I,i} \hat{n}_{Ii\uparrow} \hat{n}_{Ii\downarrow} + V \sum_{I,i;J,j} \hat{n}_{Ii} \hat{n}_{Jj}. \quad (15b)$$

The second term in Eq. (15b) contains both the intra-cluster as well as the inter-cluster V -interactions. Consider now the projection of the hopping term. In the VCGA discussed before, for a given hopping term between two sites, one can always choose a cluster coverage such that the two sites reside in two different clusters. The expectation value of the hopping term between the projected states can be evaluated according to Eq. (9). Moreover, to be consistent with the Gutzwiller approximation, the inter-cluster correlation should be ignored, which means that the inter-cluster V in Eq. (15b) should be turned off accordingly. The form of the cluster projection operator is therefore formally identical to that in Eq. (8) for the ionic Hubbard model, since the intra-cluster V -term in Eq. (15b) only leads to different energies of the multiplets in the cluster Hilbert space. An explicit example of the V -dependent cluster Fock state energies is given in Fig. 3 for the case of a two-site cluster. Consequently, the Gutzwiller hopping renormalization factors for all hopping amplitudes have the same

form and are given by Eqs. (12a) and (12b) in terms of occupation probabilities for two-site clusters. The inter-cluster V -term will take the same value since the bond becomes intra-cell under a different choice of the virtual cluster configuration. In short, the advantage of the virtual cluster formulation is that all bonds connected by hopping and the inter-site Coulomb interaction V are treated on equal footing and remain equivalent after Gutzwiller projection without artificially breaking the lattice translation symmetry.

B. Wigner-Mott transition as superstructure Mottness

We now present our results obtained for the extended Hubbard t - U - V model at quarter-filling using the VCGA with two-site clusters. Following the above discussion, the renormalized mean-field Hamiltonian in the VCGA is given by,

$$\begin{aligned} \hat{H}_{GA} = & \sum_{k,\alpha\beta} g_{\alpha\sigma} g_{\beta\sigma} \xi_{\alpha\beta}(k) c_{k,\alpha\sigma}^\dagger c_{k,\beta\sigma} \\ & + N_c U \left(\sum_{\alpha} d_{\alpha\alpha} + \sum_{\alpha\sigma} t_{\alpha\sigma} + 2f \right) \\ & + 4N_c V \left(\sum_{\sigma\sigma'} d_{\sigma\sigma'} + 2 \sum_{\alpha\sigma} t_{\alpha\sigma} + 4f \right) \\ & + \sum_{k,\alpha\sigma} \lambda_{\alpha\sigma} (\hat{n}_{k,\alpha\sigma} - n_{\alpha\sigma}), \end{aligned} \quad (16)$$

where the Gutzwiller factors are given by Eqs. (12a) and (12b) with the occupation probabilities satisfying the fermion counting and completeness equations (13a-13c). The paramagnetic ground state is obtained by minimize $\langle \hat{H}_{GA} \rangle$ with respect to the variational parameters just as in the ionic Hubbard model studied in Section III.

1. Comparison to Hartree approximation

We first demonstrate that our strong coupling, non-perturbative VCGA treatment of the inter-site correlation V is fundamentally superior to the weak-coupling Hartree approximation of the V -term with a single-site Gutzwiller projection of the on-site repulsion U . To this end, we compare the ground state energy of the quarter-filled t - U - V model at $U = W$. Fig. 6 shows that while the ground state energy obtained by VCGA is consistent with the weak coupling Hartree result for small values of V , which is in fact a nontrivial check for the validity of the VCGA, it is significantly lower for all values of V larger than about 10% of the bandwidth. The ground state energy approaches zero for $V \sim W$ in the Hartree approach, signifying a transition to the charge ordered insulating state. The result of the VCGA clearly shows that the Hartree approximation grossly overestimated the charge ordering tendency. This is because the weak-coupling Hartree-decoupling gives rise to a self-energy for

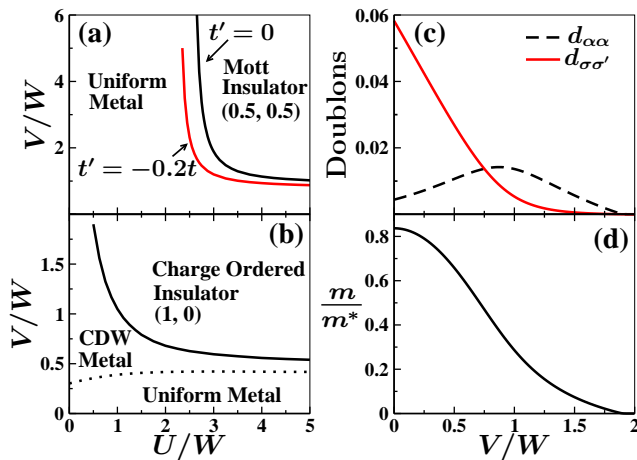


FIG. 7: (Color online) (a) Phase diagram of the t - U - V model on the U - V plane. (b) Phase diagram in the V -Hartree approximation. Doublon densities (c) and inverse effective mass (d) as functions of V at fixed $U = 3W$.

the fermions that scales with V and becomes unphysical when V is large. On the other hand, in the nonperturbative VCGA, there is no self-energy cost that scales with V . Thus the uniform metallic ground state turns out to be much more robust against inter-site correlations.

While it is clear that the results of the VCGA can be systematically improved with increasing cluster size to treat the inter-site correlations even better, we show below that it already captures the essence of the superstructure Mott metal-insulator transition with two-site supercells.

2. Wigner-Mott transition in the t - U - V model

The phase diagram obtained using the VCGA at quarter-filling is shown in Fig. 7(a) on the U - V plane. It contains a uniform strongly correlated metal at small (U, V) and a Mott insulator at large (U, V) . Since the crystal field splitting is absent, the two degenerate QP bands narrow and undergo a continuous Mott transition simultaneously upon approaching the phase boundary from the metallic side, corresponding to the first case of the superstructure Mottness transition shown in Fig. 1(a). Figs. 7(c) and 7(d) show that double occupation, the (inverse) QP mass renormalization m/m^* and the QP coherence weight decrease continuously with increasing V , which are clear signatures of Mottness, and vanish at the critical $V_c = 1.9W$ for $U = 3W$. The strongly correlated metallic phase is stable against the two-sublattice antiferromagnetic (AF) spin density wave order because the quarter-filled Fermi surface is away from the AF zone boundary. It is remarkable that for degenerate bands, the Mott transition driven by V takes place with uniform charge density without forming a Wigner lattice, suggesting that superstructure Mottness

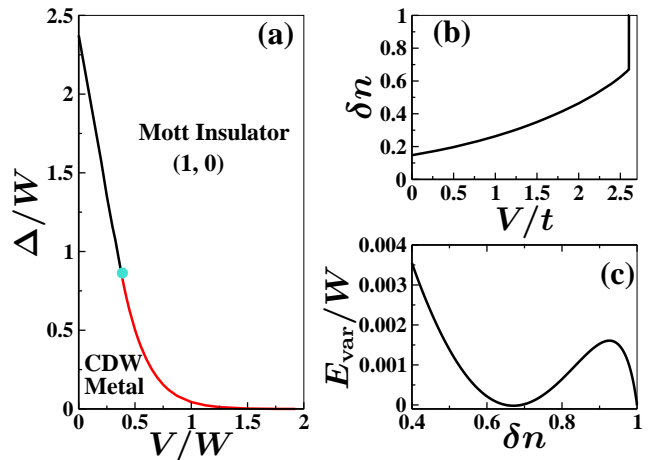


FIG. 8: (Color online) (a) Phase Diagram of the t - U - V - Δ model on the V - Δ plane at fixed $U = 3W$. The circle on the boundary separates discontinuous and continuous transitions. (b) Charge difference $\delta n = n_B - n_A$ as a function of V with $\Delta = t$ and $U = 3W$. (c) The variational energy as a function of δn at $\Delta = t$, $V = 2.6t$, and $U = 3W$.

is a more suitable description than a Wigner crystal. Since the Mott insulating state has the same energy as the (0, 1) charge ordered classical Wigner crystal, an arbitrarily small crystal field (i.e. superlattice potential) would trigger a first order transition to an orbital ordered state, corresponding to a charge ordered state in the original model. Interestingly, if the two bands have different bandwidths, corresponding to anisotropic NNN hopping $t'_A \neq t'_B$, the Mott insulating state emerges at large U and V continuously from a CDW metal with a finite density polarization δn .

It is useful to further compare these results to previous studies where the V -term is decoupled by Hartree approximation^{13,14,15}. The phase diagram in the latter case obtained by the single-site Gutzwiller approximation is shown in Fig. 7(b), where a uniform metal at small V transforms into a CDW metal and eventually to a charge ordered insulator at large V . The topology of this phase diagram is consistent with that obtained by the dynamical mean field theory at finite temperatures with a semi-circular density of states¹⁵. However, the CDW metal phase is absent in our VCGA approach that treats U and V on equal footing. It is likely that in the Hartree approximation, the fermion self-energy scaling with V overemphasizes the symmetry breaking CDW ordering tendency at large V as discussed above.

V. SUPERSTRUCTURE MOTTNESS WITH COMBINED Δ AND V

Finally, we turn to the most general case of the t - U - V - Δ model and study the interplay between the crystal field splitting Δ and the extended Coulomb interaction

V . Treating the V -term using the VCGA in the same way as in Sec. IV and putting the Δ -term in the local part of the Hamiltonian in Eq. (15b), we arrive at the identical form of the Gutzwiller renormalization factors. The only difference is that the crystal field term should be added in the renormalized mean-field Hamiltonian in Eq. (16). Fig. 8(a) displays the phase diagram at $U = 3W$ for the quarter-filled t - U - V - Δ model. In contrast to the $V = 0$ case shown in Fig. 5(a), the coherent motion in the strongly correlated metallic state is further suppressed by the inter-site correlation V such that a small (infinitesimal) Δ can drive the system to the charge ordered insulating state, provided V is large. Similarly, the superlattice potential Δ is seen to enhance the correlation effects such that the localization and local moment formation can be induced by a moderate strength of the inter-site Coulomb interaction V .

The phase boundary between the CDW metal and the charge ordered insulator in Fig. 8(a) changes from a discontinuous Wigner-Mott transition at small Δ to a continuous Brinkman-Rice transition above a critical Δ . The existence of two types of metal-insulator transition when both V and Δ are present is consistent with a recent DMFT study of a two-band Hubbard model with $U = U'$ and $\Delta \neq 0$ ³². Fig. 8(b) shows the charge density difference as a function of V at $\Delta = t$, displaying a discontinuous jump at a critical $V_c = 2.6t$. The discontinuous transition is a consequence of degenerate minima in the ground state energy for fixed (V, Δ) . In Fig. 8(c), we plot the variational ground state energy E_{var} as a function of the density difference δn at $V = 2.6t$ and $\Delta = t$ close to the phase boundary. The minimum at $\delta n = 0.67$ corresponding to a CDW metal is nearly degenerate to that of the charge ordered insulator at $\delta n = 1$. Increasing V and Δ further will make the energy of the insulating state

the global minimum and trigger the first order transition. The existence of two types of localization transition into the local moment phase is an important and unique property associated with superstructure Mottness.

VI. CONCLUSIONS

We have shown that the superlattice potential in an inhomogeneous electronic state and the inter-site Coulomb repulsion increase the correlation effect and the tendency toward localization and local moment formation. Mapping to the generic multiband Hubbard model revealed a deeper connection among the strongly correlated inhomogeneous electronic states, the Wigner-Mott physics, and the multiorbital Mott-Hubbard physics under the unified notion of superstructure Mottness. An unbiased treatment of both the on-site and inter-site Coulomb interactions, e.g. the virtual cluster approximation developed here within the framework of the Gutzwiller approximation, is essential as demonstrated for the quarter filled Hubbard model. We expect that doping away from such unconventional insulating states will further reveal behaviors of superstructure Mottness, such as the coexistence of local moment and itinerant carriers. At dilute electron densities, the competition between itinerant ferromagnetism and local moment formation may also arise due to superstructure Mottness in inhomogeneous electron systems.

We thank Hong Ding and Xi Dai for useful discussions. ZW thanks the Institute of Physics, Chinese Academy of Sciences for hospitality. This work was supported in part by DOE grant DE-FG02-99ER45747 and NSF grant DMR-0704545.

-
- ¹ G. Kotliar, S. Y. Savrasov, K. Haule, V. S. Oudovenko, O. Parcollet, C. A. Marianetti, *Rev. Mod. Phys.* **78**, 865 (2006).
- ² P. Phillips, *Ann. Phys. (N.Y.)* **321**, 1634 (2006).
- ³ P. Fazekas and E. Tosatti, *Philos. Mag. B* **39**, 229 (1979).
- ⁴ S. Colonna, F. Ronci, A. Cricenti, L. Perfetti, H. Berger, and M. Grioni, *Phys. Rev. Lett.* **94**, 036405 (2005).
- ⁵ S. A. Kivelson, I. P. Bindloss, E. Fradkin, V. Oganesyan, J. M. Tranquada, A. Kapitulnik, and C. Howald, *Rev. Mod. Phys.* **75**, 1201 (2003).
- ⁶ T. Hanaguri, C. Lupien, Y. Kohsaka, D.-H. Lee, M. Azuma, M. Takano, H. Takagi, and J. C. Davis, *Nature* **430**, 1001 (2004).
- ⁷ R. Matzdorf, Z. Fang, Ismail, Jiandi Zhang, T. Kimura, Y. Tokura, K. Terakura, and E. W. Plummer, *Science* **289**, 746 (2000).
- ⁸ M. Roger, D. J. P. Morris, D. A. Tennant, M. J. Gutmann, J. P. Goff, J.-U. Hoffmann, R. Feyerherm, E. Dudzik, D. Prabhakaran, A. T. Boothroyd, N. Shannon, B. Lake, and P. P. Deen, *Nature* **445**, 631 (2007).
- ⁹ F. C. Chou, M.-W. Chu, G. J. Shu, F.-T. Huang, Woei Wu Pai, H. S. Sheu, and Patrick A. Lee, *Phys. Rev. Lett.* **101**, 127404 (2008).
- ¹⁰ C. A. Marianetti and G. Kotliar, *Phys. Rev. Lett.* **98**, 176405 (2007).
- ¹¹ M. Gao, S. Zhou, and Z. Wang, *Phys. Rev. B* **76**, 180402(R) (2007).
- ¹² M. Neupane, P. Richard, Z.-H. Pan, Y. Xu, R. Jin, D. Mandrus, X. Dai, Z. Fang, Z. Wang, and H. Ding, arXiv:0808.0346, *Phys. Rev. Lett.* in press, (2009).
- ¹³ R. Pietig, R. Bulla, and S. Blawid, *Phys. Rev. Lett.* **82**, 4046 (1999).
- ¹⁴ Jaime Merino and Ross H. McKenzie, *Phys. Rev. Lett.* **87**, 237002 (2001).
- ¹⁵ A. Camjayi, K. Haule, V. Dobrosavljević, and G. Kotliar, *Nat. Phys.* **4**, 932 (2008).
- ¹⁶ J. Bünenmann, W. Weber and F. Gebhard, *Phys. Rev. B* **57**, 6896 (1998). R. Frésard and G. Kotliar, *Phys. Rev. B* **56**, 12909 (1997); H. Hasegawa, *Phys. Rev. B* **56**, 1196 (1997).
- ¹⁷ V. I. Anisimov, I. A. Nekrasov, D. E. Kondakov, T. M. Rice, and M. Sigrist, *Eur. Phys. J. B* **25**, 191 (2002).

- ¹⁸ C. Castellani, C. R. Natoli, and J. Ranninger, Phys. Rev. B **18**, 4945 (1978).
- ¹⁹ M. C. Gutzwiller, Phys. Rev. Lett. **10**, 159 (1963).
- ²⁰ W. Metzner and D. Vollhardt, Phys. Rev. Lett. **59**, 121 (1987); W. Metzner and D. Vollhardt, Phys. Rev. B **37**, 7382 (1988).
- ²¹ M. C. Gutzwiller, Phys. Rev. B **137**, A1726 (1965).
- ²² D. Vollhardt, Rev. Mod. Phys. **56**, 99 (1984).
- ²³ F. C. Zhang, C. Gros, T. M. Rice, and H. Shiba, Supercond. Sci. Technol. **1**, 36 (1988).
- ²⁴ C. Li and S. Zhou and Z. Wang, Phys. Rev. B **73**, 060501(R) (2006)
- ²⁵ N. Fukushima, Phys. Rev. B **78**, 115105 (2008).
- ²⁶ W. H. Ko, C. P. Nave, and P. A. Lee, Phys. Rev. B **76**, 245113 (2007).
- ²⁷ Q.-H. Wang, Z. D. Wang, Y. Chen, and F. C. Zhang, Phys. Rev. B **73**, 092507 (2006).
- ²⁸ C. Li, PhD thesis, Boston College (2009).
- ²⁹ F. Lechermann, A. Georges, G. Kotliar, and O. Parcollet Phys. Rev. B **76**, 155102 (2007).
- ³⁰ H. Yokoyama and H. Shiba, J. Phys. Soc. Jpn. **59**, 3669 (1990).
- ³¹ W. Brinkman and T. M. Rice, Phys. Rev. B **2**, 4302 (1970).
- ³² A. I. Poteryaev, M. Ferrero, A. Georges, and O. Parcollet, Phys. Rev. B **78**, 045115 (2008).